Cyclic Electron Transport around PSI Contributes to Photosynthetic Induction with Thioredoxin *f*[1][OPEN]

Yuki Okegawa,[a,b,2,3] Leonardo Basso,[c,2] Toshiharu Shikanai,[c] and Ken Motohashi[a,b,4]

[a]Department of Frontier Life Sciences, Faculty of Life Sciences, Kyoto Sangyo University, Kamigamo Motoyama, Kita-ku, Kyoto 603–8555, Japan
[b]Center for Plant Sciences, Kyoto Sangyo University, Kamigamo Motoyama, Kita-ku, Kyoto 603–8555, Japan
[c]Department of Botany, Graduate School of Science, Kyoto University, Oiwake-cho, Kitashirakawa, Sakyo-ku, Kyoto 606–8502, Japan

ORCID IDs: 0000-0001-7712-021X (Y.O.); 0000-0003-3565-9553 (L.B.); 0000-0002-6154-4728 (T.S.); 0000-0002-8414-2836 (K.M.)

In response to light, plants efficiently induce photosynthesis. Light activation of thiol enzymes by the thioredoxin (Trx) systems and cyclic electron transport by the PROTON GRADIENT REGULATION5 (PGR5)-dependent pathway contribute substantially to regulation of photosynthesis. Arabidopsis (*Arabidopsis thaliana*) mutants lacking *f*-type Trxs (*trx f1f2*) show delayed activation of carbon assimilation due to impaired photoreduction of Calvin-Benson cycle enzymes. To further study regulatory mechanisms that contribute to efficiency during the induction of photosynthesis, we analyzed the contributions of PSI donor- and acceptor-side regulation in the *trx f1f2* mutant background. The cytochrome b_6f complex is involved in PSI donor-side regulation, whereas PGR5-dependent PSI cyclic electron transport is required for both donor and acceptor functions. Introduction of the *pgr1* mutation, which is conditionally defective in cytochrome b_6f complex activity, into the *trx f1f2* mutant background did not further affect the induction of photosynthesis, but the combined deficiency of Trx *f* and PGR5 severely impaired photosynthesis and suppressed plant growth under long-day conditions. In the *pgr5 trx f1f2* mutant, the acceptor-side of PSI was almost completely reduced, and quantum yields of PSII and PSI hardly increased during the induction of photosynthesis. We also compared the photoreduction of thiol enzymes between the *trx f1f2* and *pgr5 trxf1f2* mutants. The *pgr5* mutation did not result in further impaired photoreduction of Calvin-Benson cycle enzymes or ATP synthase in the *trx f1f2* mutant background. These results indicated that acceptor-side limitations in the *pgr5 trx f1f2* mutant suppress photosynthesis initiation, suggesting that PGR5 is required for efficient photosynthesis induction.

Photosynthesis consists of a series of electron transport reactions in the thylakoid membrane and carbon fixation reactions in the stroma. In the thylakoid reactions, electrons excised from water in PSII are transferred to $NADP^+$ through the cytochrome b_6f complex and PSI, resulting in the production of NADPH. Electron transport is coupled with the translocation of protons across the thylakoid membrane from the stroma to the lumen. The resulting proton motive force (pmf) is utilized in ATP synthesis. NADPH and ATP are used to fix inorganic carbon in the Calvin-Benson cycle. In addition to this linear electron transport from water to $NADP^+$, PSI cyclic electron transport contributes to the supply of ATP for carbon fixation. PSI cyclic electron transport consists of two partially redundant pathways, namely the PROTON GRADIENT REGULATION5 (PGR5)-dependent and NADH dehydrogenase-like (NDH) complex-dependent pathways (Munekage et al., 2002, 2004; DalCorso et al., 2008). In Arabidopsis (*Arabidopsis thaliana*), the PGR5-dependent pathway is the main route for PSI cyclic electron transport and contributes to the generation of pmf across the thylakoid membrane and the resulting ATP synthesis (Munekage et al., 2002; DalCorso et al., 2008; Wang et al., 2015).

To optimize photosynthetic reactions, chloroplasts have various regulatory mechanisms (Tikhonov, 2015). The downregulation of the cytochrome b_6f complex, termed photosynthetic control, is a fundamental mechanism involved in the regulation of photosynthesis (Tikhonov, 2013). To avoid acceptor-side limitation of PSI, electron transport via the cytochrome b_6f complex is slowed through acidification of the thylakoid lumen (Stiehl and Witt, 1969). The Arabidopsis *pgr1* mutant, which has an amino acid alteration in the Rieske subunit

[1]This work was supported by the Japan Society for the Promotion of Science Grant-in-Aid for Scientific Research on Innovative Areas (grant nos. JP17H05730 and JP19H04733 to Y.O. and JP16H06552 to T.S.) and the Ministry of Education, Culture, Sports, Science, and Technology Supported Program for the Strategic Research Foundation at Private Universities (grant no. S1511023 to K.M.).

[2]These authors contributed equally to the article.

[3]Author for contact: okegawa@cc.kyoto-su.ac.jp

[4]Senior author.

The author responsible for distribution of materials integral to the findings presented in this article in accordance with the policy described in the Instructions for Authors (www.plantphysiol.org) is: Motohashi (motohas@cc.kyoto-su.ac.jp).

Y.O., L.B., and T.S. designed the research; Y.O. and L.B. performed the experiments; Y.O., L.B., T.S., and K.M. analyzed the data; and Y.O., L.B., T.S., and K.M wrote the paper.

[OPEN]Articles can be viewed without a subscription.

www.plantphysiol.org/cgi/doi/10.1104/pp.20.00741

of the cytochrome b_6f complex, has a decreased electron transport rate owing to its hypersensitivity to low luminal pH (Munekage et al., 2001; Jahns et al., 2002). Furthermore, the *pgr1* mutant cannot induce the thermal dissipation of the excess light energy absorbed by the PSII antennae, which is a photoprotective mechanism of PSII to avoid oxidative stress (Müller et al., 2001; Li et al., 2002). The sensitivity of the cytochrome b_6f complex to luminal acidification should be optimized for efficient photosynthesis and photoprotection. PSI cyclic electron transport is also important for photosynthesis and photoprotection (Munekage et al., 2004). The Arabidopsis *pgr5* mutant not only fails to induce thermal dissipation but also cannot induce photosynthetic control (Suorsa et al., 2012; Yamamoto and Shikanai, 2019).

Thioredoxin (Trx) systems also play a central role in the regulation of photosynthesis (Geigenberger and Fernie, 2014; Nikkanen and Rintamäki, 2019; Yoshida et al., 2019). In the chloroplast, there are two Trx systems; the first, classically known as the ferredoxin-Trx reductase/Trx system, depends on photoreduced ferredoxin (Fd) for reducing equivalents (Schürmann and Buchanan, 2008; Buchanan, 2016), whereas the second, the NADPH-Trx reductase C (NTRC) system, uses NADPH (Serrato et al., 2004; Pérez-Ruiz et al., 2006). Uniquely, the chloroplast-localized NTRC consists of both reductase (NTR) and Trx domains in a polypeptide (Serrato et al., 2004). Meanwhile, classical Trxs are small molecular mass proteins (~14 kD) that contain a conserved WC(G/P)PC motif in the redox-active site (Schürmann and Buchanan, 2008). Trxs reduce the disulfide bonds of target proteins and thereby regulate their activities. Arabidopsis chloroplasts contain 10 Trxs (*f*1, *f*2, *m*1, *m*2, *m*3, *m*4, *x*, *y*1, *y*2, and *z*) classified into five types (Balsera et al., 2014; Buchanan, 2016; Kang et al., 2019). Trx *m* is the most abundant type and accounts for ~69% of all Trx proteins in the chloroplast stroma (Okegawa and Motohashi, 2015). Trx *m* was demonstrated to be essential for plant growth and photoprotection, as its deficiency causes growth defects (Wang et al., 2013; Okegawa and Motohashi, 2015). Trx *f* is another major Trx; it accounts for ~22% of all Trx proteins in the stroma. Initial biochemical analyses in vitro have shown that Trx *f* plays a central role in the redox regulation of enzymes in the Calvin-Benson cycle, such as Fru-1,6-bisphosphatase (FBPase) and sedoheptulose-1,7-bisphosphatase (SBPase; Schürmann and Buchanan, 2008; Geigenberger and Fernie, 2014; Yoshida et al., 2015). However, an Arabidopsis Trx *f*-deficient mutant (termed *trx f1f2*), which lacks both Trx *f*1 and Trx *f*2, does not show any growth differences compared with the wild type under long-day conditions (Yoshida et al., 2015; Naranjo et al., 2016). In contrast, Naranjo et al. (2016) reported that the *trx f1f2* mutant does display growth inhibition under short-day conditions. They suggested that Trx *f* is dispensable for plant growth but is required for the efficient induction of photosynthesis.

Here, we characterized the *trx f1f2* double mutant, the *pgr1 trx f1f2* triple mutant (in which the cytochrome b_6f complex is hypersensitive to luminal acidification), and the *pgr5 trx f1f2* triple mutant (in which PGR5-dependent PSI cyclic electron transport is also disturbed). In the *trx f1f2* mutant, a delay in the activation of Calvin-Benson cycle enzymes during the induction of photosynthesis caused low activity of ATP synthase. Furthermore, the *pgr5 trx f1f2* triple mutant exhibited severe growth defects, suggesting that PGR5-dependent PSI cyclic electron transport is indispensable in the *trx f1f2* mutant background. We propose that PGR5-dependent PSI cyclic electron transport also contributes to efficient photosynthetic induction.

RESULTS

The *pgr5 trx f1f2* Triple Mutant Exhibited Severe Growth Defects under Long-Day Conditions

To examine the effect of the *pgr1* and *pgr5* mutations on photosynthesis in the *trx f1f2* mutant background, the triple mutants *pgr1 trx f1f2* and *pgr5 trx f1f2* were generated by crossing. Whereas the *pgr1 trx f1f2* plants were indistinguishable from the wild-type plants under long-day conditions, growth was severely affected in the *pgr5 trx f1f2* mutant (Fig. 1A; Supplemental Fig. S1A). There was no difference in the fresh weight of 3-week-old plants among the wild-type, *pgr1*, *pgr5*, *trx f1f2*, and *pgr1 trx f1f2* plants (Fig. 1B). In contrast, the fresh weight of the *pgr5 trx f1f2* plants was less than half of that of the wild-type plants (Fig. 1B). Furthermore, the chlorophyll content in the *pgr5 trx f1f2* leaves was ~58% of that in the wild-type leaves (Fig. 1C). These results indicated that the combination of the *pgr5* and *trx f1f2* mutations led to severe growth defects. Interestingly, the growth retardation in the *pgr5 trx f1f2* plants was less evident when they were grown under continuous light conditions (Supplemental Fig. S1B). The fresh weight of the *pgr5 trx f1f2* plants was ~74% of that of the wild-type plants (Supplemental Fig. S1C), and its chlorophyll content was almost the same as that of the *pgr5* mutant (Supplemental Fig. S1D). Since Trx *f* was proposed to be a requirement for the effective induction of photosynthesis (Naranjo et al., 2016), continuous light conditions may be better for the *pgr5 trx f1f2* plants.

To examine the influence of both the *pgr5* and *trx f1f2* mutations on the stability of photosynthesis-related proteins, western blot analysis was performed (Fig. 1, D and E). As reported previously (Yoshida et al., 2015), in the *trx f1f2* mutant, the protein levels of other Trx isoforms did not change (Fig. 1D). In the *pgr5 trxf1f2* mutant, the accumulation of Calvin-Benson cycle enzymes and subunits of the photosynthetic complexes were comparable to that in the wild type (Fig. 1, D and E).

The Quantum Yield of PSII Was Severely Impaired in the *pgr5 trx f1f2* Mutant

To characterize photosynthetic activity in the mutants, their chlorophyll fluorescence parameters were

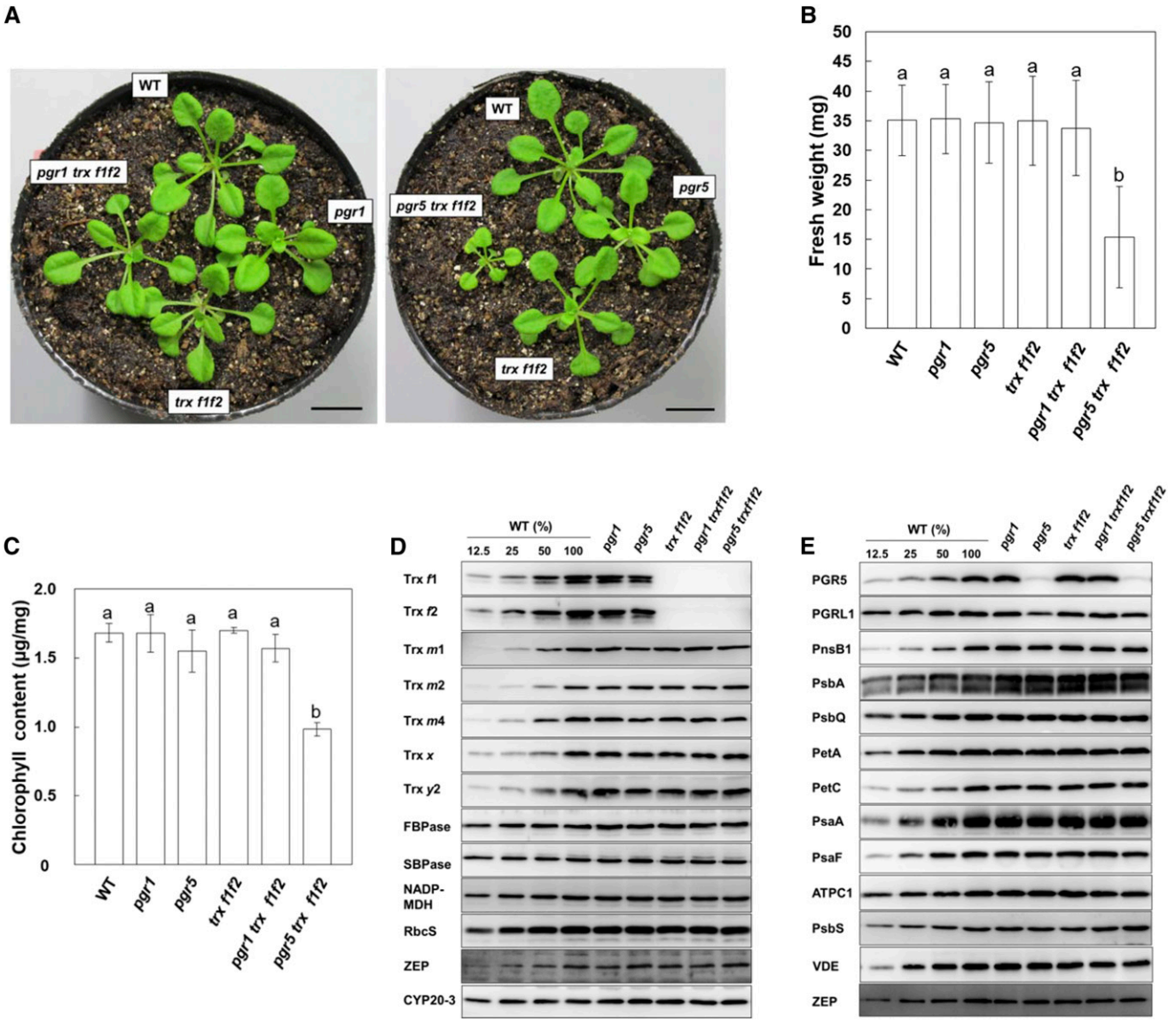

Figure 1. Visible phenotypes of the wild type (WT) and *pgr1*, *pgr5*, *trx f1f2*, *pgr1 trx f1f2*, and *pgr5 trx f1f2* mutants grown for 3 weeks under long-day conditions. A, Photographs of the plants. Bars = 10 mm. B, Fresh weights of seedlings. Each value is shown as the mean ± SD of 10 independent replicates. C, Chlorophyll content of seedlings, per unit fresh weight. Each value is the mean ± SD of three independent replicates. Columns with the same letters are not significantly different between genotypes by Tukey-Kramer test ($P < 0.05$). D and E, Western blot analysis. Chloroplasts were fractionated into the stromal fractions (D) and thylakoid membranes (E). For the wild type, dilution series of proteins corresponding to 1.0 (100%), 0.5, 0.25, and 0.125 μg chlorophyll were loaded. Other mutants contained proteins corresponding to 1.0 μg chlorophyll in each lane.

analyzed using a mini-pulse amplitude modulation (PAM) II portable chlorophyll fluorometer. The maximum quantum yield of PSII (F_v/F_m) was lower in the *pgr5 trx f1f2* mutant than in the other genotypes (Fig. 2A). To assess the functionality of PSII in the *pgr5 trx f1f2* mutant under growth light conditions, photochemical quenching in the dark (qPd) was measured according to Ruban and Murchie (2012). qPd represents the redox state of the Q_A site of PSII in the dark and is used to monitor the level of photoinhibition caused by both donor- and acceptor-side limitations of PSII (Wilson and Ruban, 2019). A qPd level less than 0.98 indicates plants to be photoinhibited (Ruban and Murchie, 2012). In the *pgr5 trx f1f2* mutant, qPd was lower than 0.98 after actinic light (AL) illumination (0.855 ± 0.061; Fig. 2B), indicating that PSII of the *pgr5 trx f1f2* mutant was photoinhibited even under constant low light conditions, although the accumulation of PSII subunits was not affected (Fig. 1E). The light intensity dependence of the effective quantum yield of PSII [Y(II)] and nonphotochemical quenching chlorophyll fluorescence (NPQ) were also measured. As reported

previously (Munekage et al., 2001, 2002), Y(II) was lower in both the *pgr1* and *pgr5* mutants than in the wild type at high light intensities (Fig. 2C). The *trx f1f2* mutant showed substantially decreased Y(II) at low light intensities, but a similar Y(II) level to that in the wild type at light intensities higher than 100 μmol photons m^{-2} s^{-1} (Fig. 2C). Moreover, a similar trend was also observed in the *pgr1 trxf1f2* mutant; here, Y(II) was lower than that in the *pgr1* mutant at low light intensities, whereas it was identical to that in the *pgr1* mutant at light intensities higher than 200 μmol photons m^{-2} s^{-1}. In contrast, Y(II) remained lower in the *pgr5 trx f1f2* mutant under all light intensities, compared to that in the *pgr5* and *trxf1f2* mutants (Fig. 2C).

The NPQ level mainly reflects the size of thermal dissipation in plants. The ΔpH-dependent component of NPQ (qE) was induced in the wild type at light intensities higher than 50 μmol photons m^{-2} s^{-1} (Fig. 2D). In the *pgr1* and *pgr5* single mutants, the decreased ΔpH caused a low NPQ level. In contrast, the *trx f1f2* mutant showed higher NPQ than the wild type. In the *pgr1 trx f1f2* mutant, the NPQ was slightly higher at low light intensities than that in the *pgr1* mutant (Fig. 2D). Unexpectedly, the *pgr5 trx f1f2* mutant induced a higher NPQ, especially at low light intensities, compared to that in the wild type, and the level was almost identical to that in the *trx f1f2* mutant (Fig. 2D).

In the analysis of light intensity dependence, the AL intensity was increased in a step-wise manner at every 2 min after applying a saturating pulse (SP). Since Trx *f* has been suggested to function in the activation of photosynthesis (Naranjo et al., 2016), photosynthesis may not have been activated in the *trx f1f2* mutant background at low light intensities. To evaluate this possibility, Y(II) and NPQ were assessed during the induction of photosynthesis at a low light intensity of 75 μmol photons m^{-2} s^{-1} (Fig. 2, E and F). Y(II) reached the steady-state level within 5 min after the onset of AL in the wild type. In the *trx f1f2* mutant, however, it took more than 10 min for Y(II) to reach a steady-state level, but the final value was almost identical to that in the wild type (Fig. 2E). The *pgr5 trx f1f2* mutant showed markedly lower Y(II) than the *pgr5* mutant, and the Y(II) did not increase at all even 20 min after the onset of AL (Fig. 2E). This result was consistent with the growth defect of the *pgr5 trx f1 f2* mutant (Fig. 1, A and B).

Consistent with the result of the light intensity dependence analysis (Fig. 2D), the *pgr5 trxf1f2* mutant induced a higher NPQ than the wild type (Fig. 2F). The qE component of NPQ is characterized by its relatively fast relaxation kinetics on a physiological time scale of seconds to several minutes (Horton et al., 1996). The majority of NPQ induced in the *pgr5 trx f1f2* mutant was relaxed within several minutes in the dark (Fig. 2F). These results indicated that NPQ in the *pgr5 trx f1f2* mutant was largely dependent on the qE component, suggesting that the restoration of NPQ in the *pgr5 trx f1f2* mutant is attributed to a concomitant restoration of ΔpH.

We also measured linear electron transport to $NADP^+$ in ruptured chloroplasts (Fig. 2G). Fd and $NADP^+$ were added exogenously as electron acceptors to ruptured chloroplasts. The *pgr1* mutant showed lower Y(II) than the wild type at a light intensity of 167 μmol photons m^{-2} s^{-1} owing to its hypersensitivity to low luminal pH (Munekage et al., 2001; Jahns et al., 2002), whereas the *pgr1 trx f1f2* mutant had the same Y(II) as the *pgr1* mutant (Fig. 2G). In contrast, there was no difference in the Y(II) values among the wild type and *pgr5*, *trx f1f2*, and *pgr5 trx f1f2* mutants (Fig. 2G). These results indicated that the PSII and PSI activities were not affected in the *trx f1f2* mutant background, suggesting that the markedly decreased Y(II) in the *pgr5 trx f1f2* mutant was caused by acceptor-side, but not donor-side, limitations of PSI.

The Acceptor Side of PSI Was Highly Reduced in the *pgr5 trx f1f2* Mutant Even at Low Light Intensity

The *pgr5 trxf1f2* mutant was suggested to be limited on the acceptor side of PSI. Therefore, we next simultaneously measured the chlorophyll fluorescence and absorption changes in P700 using a dual-PAM-100 system (Fig. 3). Plants were dark adapted for 30 min and then illuminated with AL (75 μmol photons m^{-2} s^{-1}) for 5 min. The Y(I) parameter is defined by the fraction of P700 that is reduced and not limited by the acceptor side (Klughammer and Schreiber, 2008) and is often used to estimate the effective quantum yield of PSI. In the wild type, Y(I) and Y(II) rapidly increased after a shift from dark to light (Fig. 3, A and B). As reported previously (Naranjo et al., 2016), in the *trx f1f2* mutant, the initial increases in Y(I) and Y(II) were markedly delayed compared with those in the wild type, and high NPQ was maintained over time (Fig. 3, A, B, and E). This was accompanied by a delay in the relaxation of the acceptor-side limitation of PSI monitored based on Y(NA) (Fig. 3C). Most likely, this phenotype was due to delayed activation of Calvin-Benson cycle enzymes followed by a shortage of electron acceptors in the *trx f1f2* mutant. Y(ND), the PSI donor-side limitation in electron transport, is used to estimate the operation of photosynthetic control. In the *pgr1* mutant, the transient peak of Y(ND) formed within 60 s of AL onset was higher than that in the wild type owing to enhanced photosynthetic control (Fig. 3D). In contrast, the *trx f1f2* mutant did not form this peak; instead, a gradual rise in Y(ND) was observed, peaking at 3 min after the onset of AL. This suggested that the thylakoid lumen became acidic during this period. The introduction of the *pgr1* mutation into the *trx f1f2* mutant background did not substantially affect its PSII or PSI photochemistry, though NPQ was partially induced even in the *pgr1* mutant background (Fig. 3E). PGR5-dependent PSI cyclic electron transport is required to protect the stroma from over-reduction (Munekage et al., 2002; DalCorso et al., 2008). In the *pgr5* mutant, the $P700^+$ level was drastically reduced at high light intensities (Supplemental Fig. S2). Even under the low light intensity used in this study, the relaxation of Y(NA) was markedly delayed in the *pgr5* mutant (Fig. 3C). The increase in Y(I) was also delayed, but it

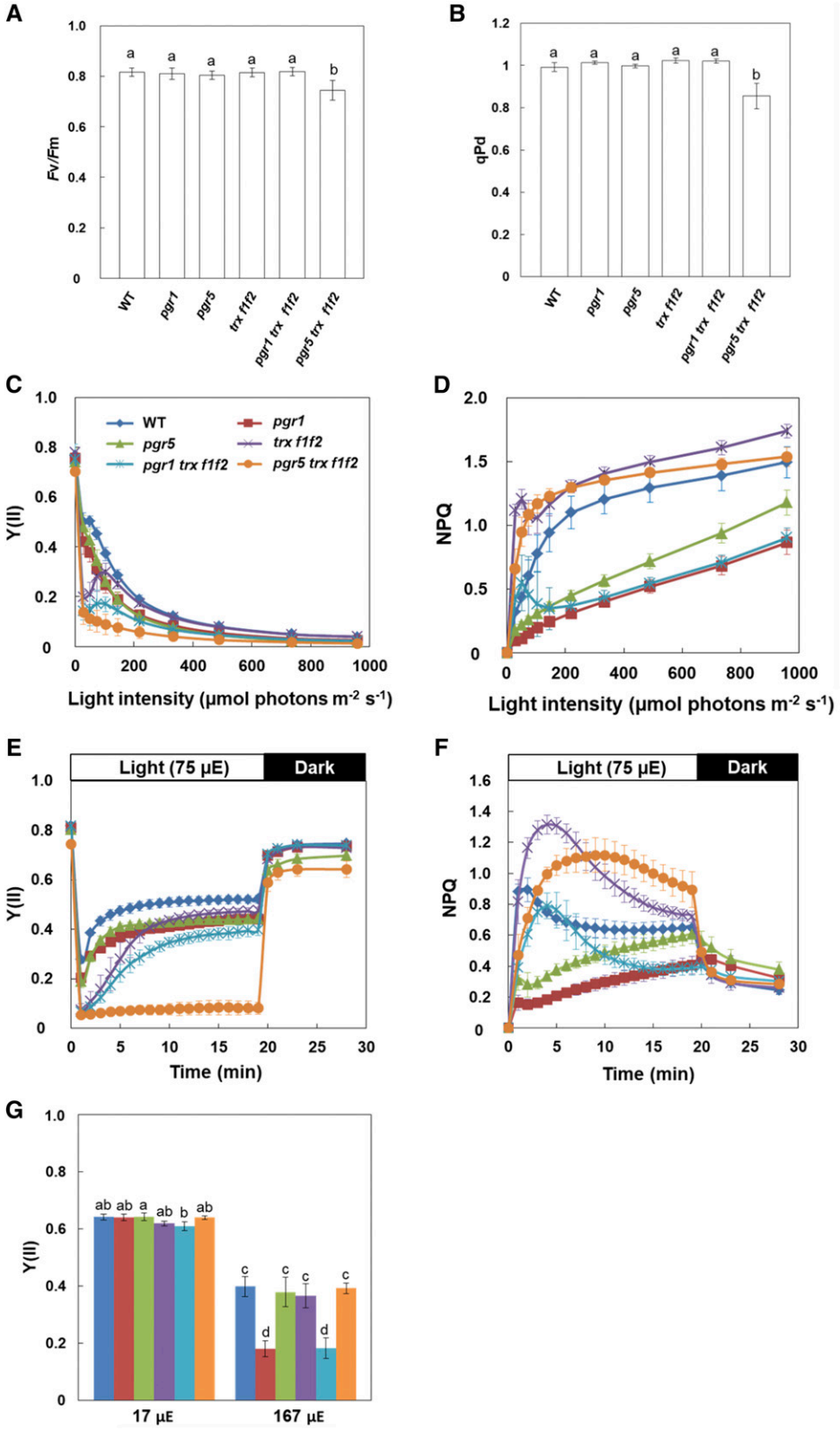

Figure 2. Chlorophyll fluorescence analysis in the wild type (WT) and *pgr1*, *pgr5*, *trx f1f2*, *pgr1 trx f1f2*, and *pgr5 trx f1f2* mutants. A, The F_v/F_m. B, qPd. qPd was determined after illumination at 50 μmol photons m^{-2} s^{-1} (growth light) for 15 min. Each value is the mean ± SD of five independent replicates. Columns with the same letters are not significantly different between genotypes by Tukey-Kramer test ($P < 0.05$). C and D, Light intensity dependence of the Y(II) and the NPQ of chlorophyll fluorescence. Each value is the mean ± SD of five independent replicates. E and F, Time courses of Y(II) and NPQ during the induction of photosynthesis. The Y(II) and NPQ values were measured upon illumination at 75 μmol photons m^{-2} s^{-1} for 20 min, followed by 8 min in the dark. Each data point represents the mean ± SD ($n = 5$ independent plants). G, Linear electron transport in ruptured chloroplasts. Y(II) was determined in ruptured chloroplasts at light intensities of 17 and 167 μmol photons m^{-2} s^{-1} (μE). Each value is the mean ± SD of three independent chloroplast preparations. Columns with the same letters are not significantly different between genotypes by Tukey-Kramer test ($P < 0.05$).

reached the wild-type level within 3 min of AL onset (Fig. 3A). In contrast, the increases in Y(I) and Y(II) were severely suppressed in the *pgr5 trx f1f2* mutant during the induction of photosynthesis (Fig. 3, A and B). The high level of Y(NA) was not relaxed at all during the 5 min of illumination (Fig. 3C). Consequently, Y(ND) was close to zero, indicating that the acceptor side of PSI was largely reduced in the *pgr5 trx f1f2* mutant, even under low light conditions. These results indicated that a combination of *pgr5* and *trx f1f2* mutations synergistically disturbed the initiation of photosynthesis.

The high level of Y(NA) in the *pgr5 trx f1f2* mutant was not relaxed within 5 min of AL onset (Fig. 3C). To determine whether this acceptor-side limitation could be observed during steady-state photosynthesis, PSI and PSII photosynthetic parameters were measured without dark adaptation (Supplemental Fig. S3). In contrast to that in the induction phase of photosynthesis, no difference in the photosynthetic parameters was observed between the wild type and *trx f1f2* mutant (Fig. 3; Supplemental Fig. S3), indicating that Trx *f* deficiency does not affect photosynthesis under steady-state conditions. At this light intensity (75 μmol photons m^{-2} s^{-1}), the parameters in the *pgr5* mutant were almost the same as those in the wild type. In contrast, in the *pgr5 trx f1f2* mutant, Y(I) was only slightly increased and high Y(NA) was only slightly relaxed, compared to those in the induction phase of photosynthesis (Fig. 3; Supplemental Fig. S3). These results suggest that PGR5-dependent PSI cyclic electron transport is required to prevent overreduction of the PSI acceptor side, especially in the *trx f1f2* mutant background, even under constant low light conditions.

The Relaxation of pmf Was Delayed in the *trx f1f2* Mutant

The *trx f1f2* mutant exhibited the induction of higher NPQ than the wild type (Figs. 2D and 3E). Furthermore, NPQ was also higher in the *pgr1 trxf1f2* and *pgr5 trx f1f2* mutants than in the *pgr1* and *pgr5* single mutants, respectively (Figs. 2D and 3E). To investigate the reason for this increase in NPQ in the *trx f1f2* mutant background, the electrochromic shift (ECS) was analyzed using a dual-PAM system. The ECS signal represents an absorbance change at 515 nm owing to photosynthetic pigments, which is affected by the electric field formed across the thylakoid membrane. ECS_t is the light-dark difference in the ECS signal and represents the magnitude of the pmf formed in the light. ECS_t was standardized against ECS_{ST}, which is the ECS signal induced by a single turnover light pulse using dark-adapted leaves. The g_{H^+} parameter is determined by monitoring the decay kinetics of the ECS signal in the dark and is considered to mainly represent the proton conductivity of ATP synthase (Takizawa et al., 2008), although the careful inspection is needed for the mutants including *pgr1* and *pgr5* (Yamamoto and Shikanai, 2020). During the induction of photosynthesis, in the wild type, high-level pmf was transiently formed, decreasing to the steady-state level within 3 min of AL onset (Fig. 4A). Conversely, g_{H^+} increased during the induction of photosynthesis, mainly reflecting the activation of chloroplast ATP synthase (Fig. 4B). This process corresponded with the induction and relaxation of NPQ (Fig. 3E). The increase in g_{H^+} was suppressed in the *trx f1f2* mutant compared to that in the wild type, resulting in delayed relaxation of the transiently induced pmf (Fig. 4). The high-NPQ phenotype observed in the *trx f1f2* mutant is probably explained by the suppression of ATP synthase activity. In the *pgr1* mutant background, the *trx f1f2* defects also enhanced pmf and lowered g_{H^+} (Fig. 4), consequently inducing higher NPQ than that in the *pgr1* mutant (Fig. 3E). In contrast, the *pgr5* mutation further decreased the g_{H^+} level in the *trx f1f2* mutant background during the period 150 to 270 s after the onset of AL (Fig. 4B). The *pgr5 trx f1f2* triple mutant did not exhibit the induction of transient NPQ (Fig. 3E), and the level of pmf after 270 s of AL onset was similar to the wild-type level and lower than the level observed in the *trx f1f2* mutant (Fig. 4A). This is probably because of the very low level of linear electron transport (Fig. 3, A and B). Despite the constantly low pmf level, the *pgr5 trx f1f2* mutant induced a moderate NPQ level (Fig. 3E). A similar trend was also observed when the light intensity dependence of these parameters was analyzed (Supplemental Fig. S4). The *pgr5 trx f1f2* mutant showed low pmf similar to that in the *pgr5* mutant but induced a higher NPQ than the *pgr5* mutant (Supplemental Fig. S2E).

Photoactivation of FBPase and SBPase Was Delayed in the *trx f1f2* Mutant

In the *trx f1f2* mutant, the g_{H^+} was lower than that in the wild type (Fig. 4B). ATP synthase in chloroplasts is light activated via reduction of the CF_1-γ subunit (Nalin and McCarty, 1984). Trx *f* contributes to the light-dependent reduction of thiol enzymes, including ATP synthase and Calvin-Benson cycle enzymes (Schwarz et al., 1997). The lower g_{H^+} might have reflected the impaired light-dependent reduction of ATP synthase. To investigate this possibility, we examined the redox state of several thiol enzymes during the induction of photosynthesis and under constant low light conditions (80 μmol photons m^{-2} s^{-1}). The thiol enzyme levels in the *trx f1f2* mutant background were not affected (Fig. 1, D and E). The light-induced state changes in the CF_1-γ subunit were determined by labeling the free thiols with the thiol-reactive 4-acetamido-4′-maleimidylstilbene-2,2′-disulfonic acid rea gent. In the wild type, CF_1-γ was rapidly reduced upon illumination from zero to the steady-state level over 300 s (Fig. 5A). This occurred in all the genotypes (Fig. 5A), suggesting that the lower level of g_{H^+} in the *trx f1f2* mutant background was not caused by the suppressed activation of ATP synthase due to the impaired reduction of CF_1-γ. As reported previously (Naranjo et al., 2016), however, the light-dependent reduction of FBPase was delayed and the final reduction level was lower in the *trx f1f2* mutant background (Fig. 5B). In the wild type, FBPase was gradually reduced within 30 s of the onset of illumination, whereas 300 s was required to start reducing FBPase in

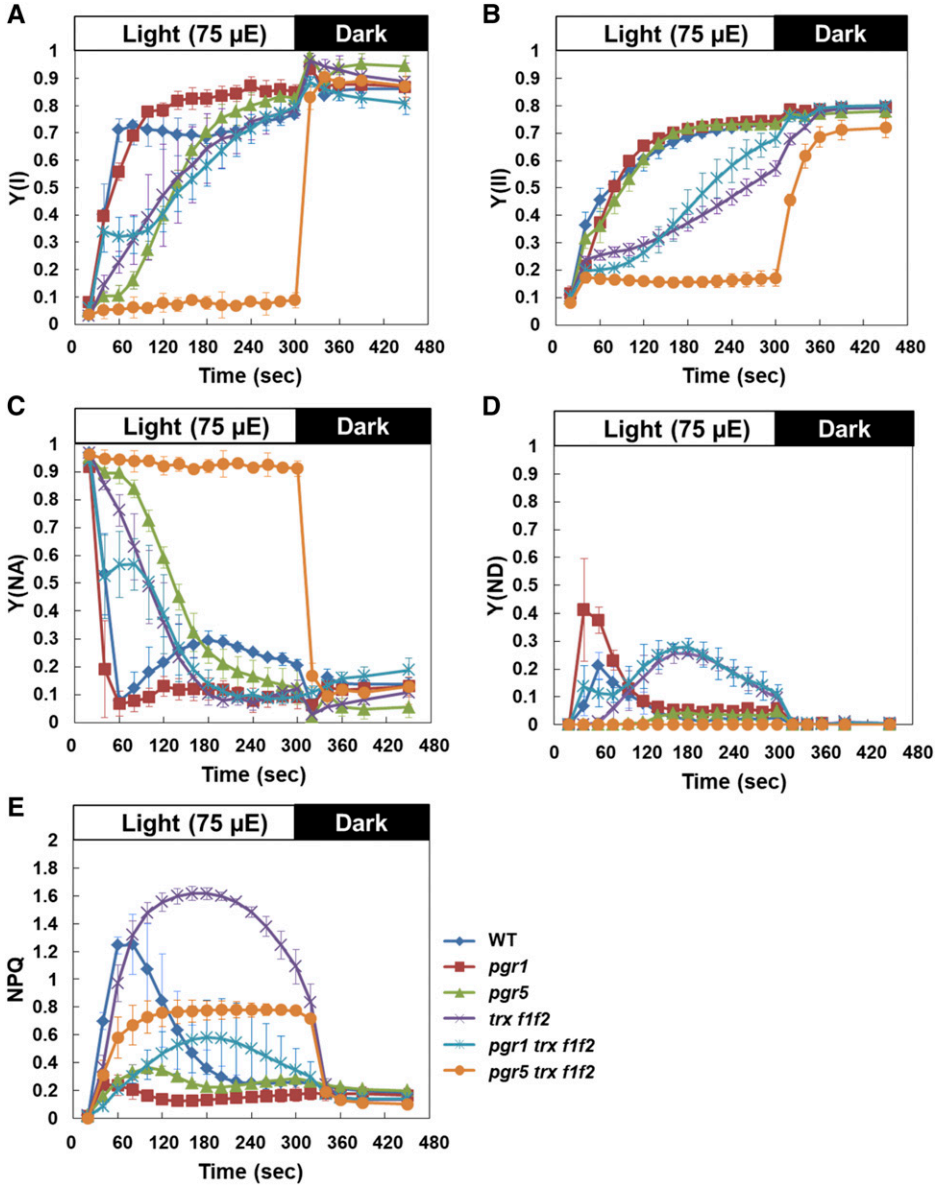

Figure 3. Simultaneous analysis of PSI and PSII photosynthetic parameters in the wild type (WT) and *pgr1*, *pgr5*, *trx f1f2*, *pgr1 trx f1f2*, and *pgr5 trx f1f2* mutants. Photosynthetic parameters were monitored under the induction of photosynthesis at a light intensity of 75 μmol photons m^{-2} s^{-1} (μE). A, Y(I). B, Y(II). C, Y(NA). D, Y(ND). E, NPQ of chlorophyll fluorescence. Plants were dark-adapted for 30 min before measurements. Each value is the mean ± SD of three independent replicates.

the *trx f1f2* mutant background (Fig. 5B). SBPase also needs to be photoreduced to be active. Compared with that of FBPase, the reduction of SBPase was slower even in the wild type (Fig. 5C). As observed for FBPase, the reduction of SBPase was delayed in the *trx f1f2* mutant background, but the final reduction level was almost

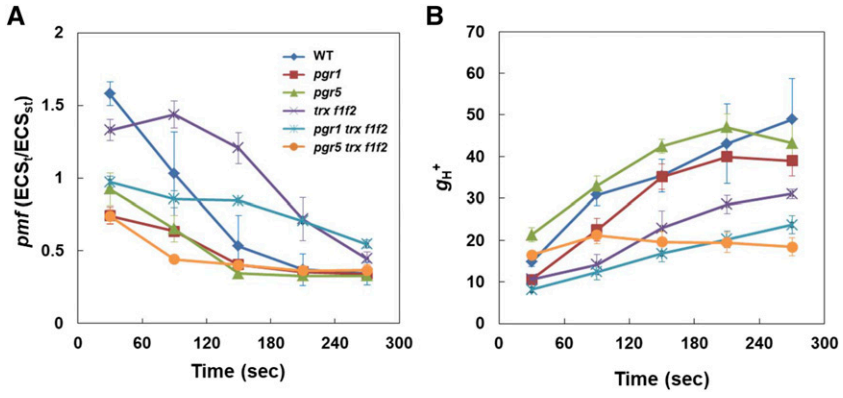

Figure 4. ECS analysis in the wild type (WT) and *pgr1*, *pgr5*, *trx f1f2*, *pgr1 trx f1f2*, and *pgr5 trx f1f2* mutants. A, Total size of pmf determined as ECS_t/ECS_{ST}. ECS_t is the light-dark difference in the ECS signal and represents the magnitude of the pmf formed in the light. ECS_{ST} signal was produced by a single turnover light pulse using dark-adapted leaves. B, Proton conductivity of the thylakoid membrane (g_{H^+}). Measurements were performed under the induction of photosynthesis at a light intensity of 75 photons m^{-2} s^{-1}. Each value is the mean ± SD of three independent replicates.

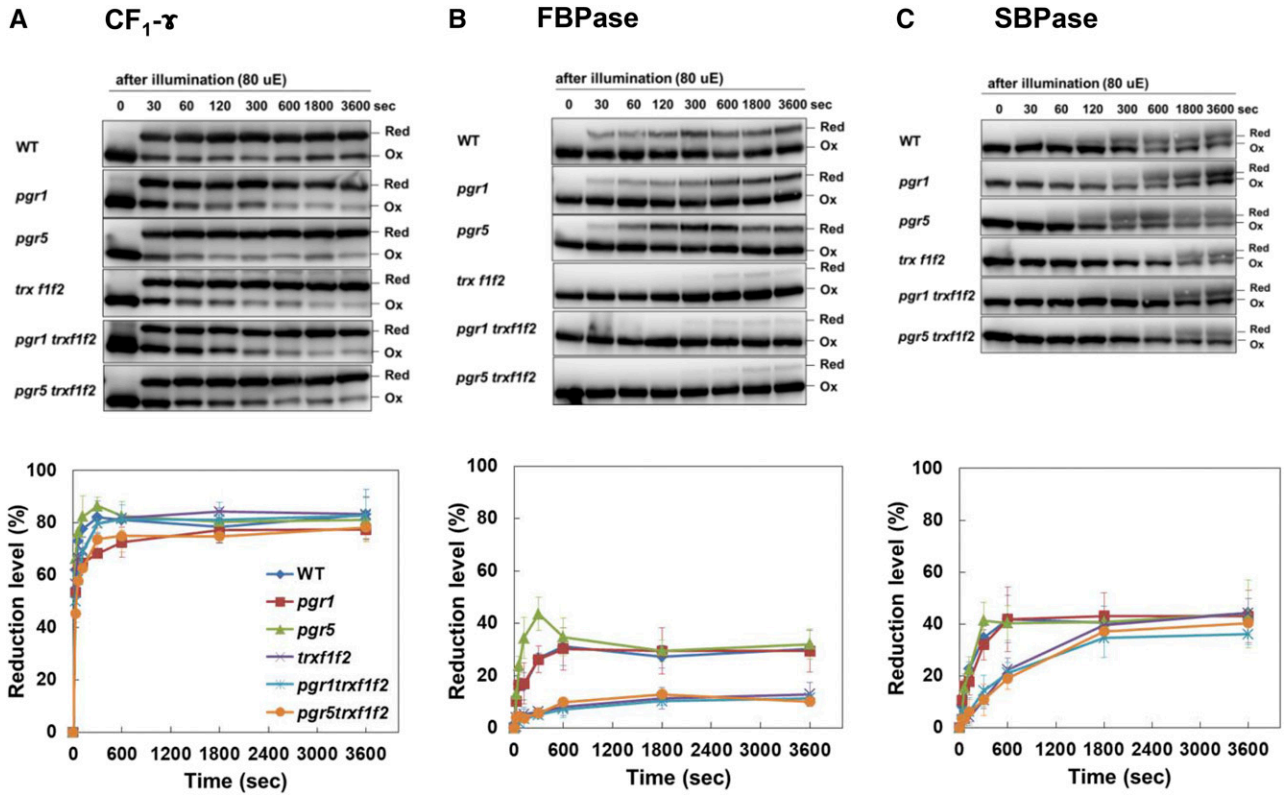

Figure 5. Photoreduction of thiol enzymes in the wild type (WT) and *pgr1*, *pgr5*, *trx f1f2*, *pgr1 trx f1f2*, and *pgr5 trx f1f2* mutants. Seedlings were illuminated at a light intensity of 80 μmol photons m^{-2} s^{-1} (μE) after a dark period of 8 h and collected at the indicated time points. The extracted proteins were modified with the thiol-reactive 4-acetamido-4′-maleimidylstilbene-2,2′-disulfonic acid and subjected to nonreducing SDS-PAGE. The redox states of ATP synthase CF_1-γ (A), FBPase (B), and SBPase (C) were detected by western blot analysis. The reduction levels of thiol enzymes were indicated as a percentage of the total protein that was reduced. Each value represents the mean ± SD of three independent replicates. Red, Reduced; Ox, oxidized.

identical to that in the wild type (Fig. 5C). Consistent with a previous report (Naranjo et al., 2016), these results indicated that Trx *f* is particularly important for the activation of Calvin-Benson cycle enzymes during the induction of photosynthesis. The low g_{H^+} in the *trx f1f2* mutant was suggested to be indirectly caused by the delayed activation of the Calvin-Benson cycle. In the *pgr1 trx f1f2* and *pgr5 trx f1f2* triple mutants, the reduction of FBPase and SBPase was delayed, as in the *trx f1f2* mutant, but their reduction levels were not further suppressed (Fig. 5, B and C). These results suggested that the higher Y(NA) and lower Y(I) and Y(II) phenotypes observed in the *pgr5 trx f1f2* triple mutant were not caused by differences in the reduction of thiol enzymes related to the *trx f1f2* mutations.

DISCUSSION

PGR5-Dependent PSI Cyclic Electron Transport Is Required for Normal Plant Growth in the *trx f1f2* Mutant Background

Here, we applied a genetic approach to evaluate the influence of PSI donor- and acceptor-side limitations on the function of Trx *f*. The *pgr1* and *pgr5* mutants exhibited a similar phenotype, with low ETR and NPQ values, but these mutations had distinct effects in the *trx f1f2* mutant background. The combination of the *pgr1* and *trx f1f2* mutations did not affect plant growth; instead, the *pgr1 trx f1f2* mutant showed a more rapid increase in Y(I) and relaxation of Y(NA) in the 40 to 100 s period after the onset of AL compared to those in the *trx f1f2* mutant (Fig. 3). These results suggest that the donor-side limitation of PSI in the *pgr1* mutant partially alleviated the acceptor-side limitation of PSI in the *trx f1f2* mutant. In contrast to that with the *pgr1* mutation, the introduction of the *pgr5* mutation into the *trx f1f2* mutant background caused severe growth defects (Fig. 1). In the *pgr5 trx f1f2* mutant, the values of Y(I) and Y(II) were markedly lower, and that of Y(NA) was substantially higher than the values in the *pgr5* and *trx f1f2* mutants, even under low light conditions (Fig. 3; Supplemental Fig. S2). This indicated that the acceptor limitation of PSI was synergistically enhanced in the *pgr5 trx f1f2* mutant. The introduction of the *pgr5* mutation into the *chlororespiratory reduction2-2* (*crr2-2*) mutant background also leads to severe growth defects (Munekage et al., 2004). The *crr2-2* mutant is deficient in

the NDH complex-dependent pathway owing to the lack of expression of the *ndhB* gene (Hashimoto et al., 2003). Recently, the activity of the NDH complex was proposed to be regulated by the Trx systems (Courteille et al., 2013; Nikkanen et al., 2018). Nikkanen et al. (2018) reported that NTRC interacts with NdhH, PnsB1 (Ndh48), NdhS, NdhU, and NdhO, which are subunits of the NDH complex, and the overexpression of NTRC enhances NDH activity. Conversely, Trx *m*4 was suggested to down-regulate NDH activity (Courteille et al., 2013). However, in contrast to the *crr2-2 pgr5* mutant, which cannot induce NPQ (Munekage et al., 2004), the *pgr5 trx f1f2* mutant induced a higher NPQ (Fig. 2D). Furthermore, the introduction of the *crr2-2* mutation into the weak mutant allele of *pgr5* further lowered pmf (Nakano et al., 2019), but the *pgr5 trx f1f2* mutant showed a similar level of pmf as the *pgr5* mutant (Supplemental Fig. S4). These results suggest that NDH activity is not affected in the *trx f1f2* mutant background and that the phenotype of the *pgr5 trx f1f2* mutant is not due to a lack of NDH complex-dependent PSI cyclic electron transport, unlike that with the *crr2-2 pgr5* mutant.

A study on the *high cyclic electron flow1* (*hcef1*) mutant, defective in FBPase, showed that the loss of FBPase activity leads to enhancement of NDH complex-dependent PSI cyclic electron transport (Livingston et al., 2010). In the *hcef1* mutant, the levels of NDH subunits were enhanced and NDH activity was stimulated. Although FBPase was less active in the *trx f1f2* mutant than in the wild type (Fig. 5B), the level of the NDH subunit (PnsB1) did not change (Fig. 1E). These results suggest the distinctly different responses of the NDH complex to the *hcef1* and *trx f1f2* mutations. Since the protein level of FBPase did not decrease in the *trx f1f2* mutant (Fig. 1D), other Trx systems could partially compensate in terms of the activation of FBPase. In fact, in the *trx f1f2* mutant, the photoreduction rate of FBPase reached approximately 40% of that in the wild type during steady-state photosynthesis (Fig. 5B). Trx *m* has also been suggested to contribute to the activation of FBPase in vivo (Okegawa and Motohashi, 2015).

Unexpectedly, the *pgr5 trxf1f2* mutant induced a higher NPQ than the *pgr5* mutant (Figs. 2, D and F, and3E). The *trx f1f2* mutant also exhibited higher NPQ than the wild type, especially during the induction of photosynthesis (Figs. 2F and 3E). In the *trx f1f2* mutant, the activation of Calvin-Benson cycle enzymes was delayed during the induction of photosynthesis, though ATP synthase was activated at the same time as that in the wild type (Fig. 5). The suppression of Calvin-Benson cycle activation may indirectly lower the activity of ATP synthase, resulting in a decreased g_{H^+} and an increased pmf in the *trx f1f2* mutant (Fig. 4). The similar phenotype was also observed in the wild type, when the CO_2 concentration was lowered and the activity of the Calvin-Benson cycle was suppressed (Avenson et al., 2005). Lowering CO_2 causes a decrease in g_{H^+}, resulting in an increase in both pmf and NPQ (Avenson et al., 2005). The *trx f1f2* mutations substantially decreased g_{H^+} in the *pgr5* mutant background (Fig. 4; Supplemental Fig. S4). However, the *pgr5 trx f1f2* mutant had a lower pmf level than the wild type, which was similar to that in the *pgr5* mutant, (Fig. 4; Supplemental Fig. S4), probably due to markedly decreased electron transport activity (Fig. 3, A and B). It is still unclear why the *pgr5 trx f1f2* mutant induced a higher NPQ than the *pgr5* mutant despite the low pmf. To explain this NPQ phenotype, we might have to consider the larger contribution of ΔpH to pmf. In the *pgr5* mutant, the contribution of ΔpH to pmf was reported to be larger than that in the wild type (Shikanai and Yamamoto, 2017). A slight change in the ratio of pmf components may lead to higher NPQ induction in the *pgr5 trx f1f2* mutant. Meanwhile, it may be dangerous to absolutely rely on the ECS signals, especially in the mutants (Yamamoto and Shikanai, 2020). The steady-state ECS signal overlaps with the absorption change at 505 nm caused by zeaxanthin synthesis and the absorption change at 535 nm caused by qE induction (Johnson and Ruban, 2014). Overall, our results indicated that donor-side limitation of PSI had no additional effect on the *trx f1f2* mutation, but acceptor-side limitation of PSI enhanced the phenotypic effects of the *trx f1f2* mutations. This suggests that PGR5-dependent PSI cyclic electron transport is needed for plant growth in the *trx f1f2* mutant background.

PGR5-Dependent PSI Cyclic Electron Transport Is Required for the Induction of Photosynthesis in the *trx f1f2* Mutant Background

The growth defects of the *pgr5 trx f1f2* mutant were partially alleviated by growing the plants under continuous light conditions (Fig. 1; Supplemental Fig. S1). This result is consistent with a previous report indicating that the *trx f1f2* mutant shows growth inhibition under short-day, but not long-day, conditions (Naranjo et al., 2016). Since the induction of photosynthesis was delayed owing to retardation in the activation of Calvin-Benson cycle enzymes in the *trx f1f2* mutant background (Figs. 3 and 5; Naranjo et al., 2016), a shorter day length would be deleterious for the *trx f1f2* mutant background plants. During steady-state photosynthesis, the *trx f1f2* mutant and wild type showed similar photosynthetic parameter levels (Supplemental Fig. S3). However, in the *pgr5 trx f1f2* mutant, Y(II) remained very low also during steady-state photosynthesis, although the Y(I) and Y(NA) values recovered slightly, compared to those in the induction phase of photosynthesis (Fig. 3; Supplemental Fig. S3). These results indicated that continuous light conditions slightly relaxed the acceptor-side limitation of PSI, resulting in the alleviation of growth defects in the *pgr5 trx f1f2* mutant (Supplemental Fig. S1, B–E). In the *pgr5 trx f1f2* mutant, the thiol enzymes were activated during steady-state photosynthesis, although the reduction level of FBPase was as low as that in the *trx f1f2* mutant (Fig. 5). Therefore, continuous light would be suitable

for the growth of the *pgr5 trx f1f2* plants. However, since PGR5-dependent PSI cyclic electron transport is more important to protect PSI under high light conditions (Munekage et al., 2002), the *pgr5 trx f1f2* mutant may show more severe growth defects when grown at higher light intensities, even under continuous light conditions.

The *ntrc trx f1* double mutant also exhibits severe growth defects (Thormählen et al., 2015; Nikkanen et al., 2016). In this mutant, the light activation of FBPase and ADP-Glc pyrophosphorylase was almost completely suppressed and the NADPH/$NADP^+$ ratio was increased (Thormählen et al., 2015). NTRC has been suggested to contribute to photosynthetic metabolism, especially under low light conditions (Carrillo et al., 2016). As NTRC uses NADPH as an electron donor, NTRC deficiency may enhance the reduction state of the stroma in the *trx f1* mutant background. In fact, photoinhibition of PSI was observed in the *ntrc trxf1* mutant (Thormählen et al., 2015). Furthermore, compared to that in the wild type, the *ntrc trx f1* mutant showed increased activation of NADP-malate dehydrogenase, which reflects the stromal redox state (Foyer et al., 1992). This indicated that the acceptor-side of PSI was limited in the *ntrc trx f1* mutant. Together with the results in the *pgr5 trx f1f2* mutant, these results suggest that the acceptor-side limitation of PSI leads to the impaired activation of photosynthesis, resulting in plant growth defects. In the *pgr5* single mutant, the induction of photosynthesis was only delayed compared to that in the wild type, at least under the low light conditions used in this study. However, in the *trx f1f2* mutant background, the *pgr5* mutation markedly suppressed photosynthetic activity. We propose that PGR5-dependent PSI cyclic electron transport is required to induce photosynthesis effectively by preventing overreduction of the stroma. Since PSI cyclic electron transport has been proposed to be regulated by the availability of electron acceptors from PSI (Breyton et al., 2006; Okegawa et al., 2008), the function of PGR5-dependent PSI cyclic electron transport in maintaining stromal redox states may become more evident in the *trx f1f2* mutant background.

MATERIALS AND METHODS

Plant Materials and Growth Conditions

Arabidopsis (*Arabidopsis thaliana*) ecotype Columbia 0 was used as the wild type. The transfer DNA (T-DNA) insertion lines SALK_128365 (*trx f1*; Thormählen et al., 2013) and GK-020E05 (*trx f2*; Yoshida et al., 2015) were obtained from the Nottingham Arabidopsis Stock Center. To generate a double mutant, *trx f1* and *trx f2* T-DNA single mutants were crossed. The triple homozygous mutants, *pgr1 trx f1f2* and *pgr5 trx f1f2*, were obtained by crossing the *trx f1f2* mutant with the *pgr1* or *pgr5* mutant, respectively. The presence of mutations and T-DNA insertions was confirmed using PCR (for primers, see Supplemental Table S1).

Plants were grown in soil or in petri dishes containing Murashige and Skoog medium with 1.0% (w/v) agar and 1% (w/v) Suc and grown for 3 to 5 weeks in growth chambers (50 μmol photons m^{-2} s^{-1}, 16 h light/8 h dark cycles or continuous light, 23°C).

Analysis of Chlorophyll Content

Leaves (30 mg fresh weight) were harvested from 3-week-old seedlings grown on Murashige and Skoog plates and immediately powdered by grinding in liquid nitrogen. Chlorophyll was extracted in 80% (v/v) acetone and collected by centrifugation at 15,000*g* for 5 min at 4°C. The residue was re-extracted with 80% (v/v) acetone and centrifuged once again (15,000*g*, 5 min, 4°C). The chlorophyll content was determined via spectrophotometry, as described previously (Porra et al., 1989).

Isolation of Chloroplasts

Chloroplasts were isolated from leaf tissue samples (1.0 g) using a Polytron PT 10-35 GT homogenizer (Kinematica) in 20 mM Tricine-NaOH, pH 8.4, containing 400 mM sorbitol, 5 mM $MgCl_2$, 5 mM $MnCl_2$, 2 mM EDTA, 10 mM $NaHCO_3$, 0.5% (w/v) bovine serum albumin, and 5 mM ascorbate. After centrifugation at 3000*g* for 5 min (4°C), the pellet was gently resuspended in 50 mM HEPES-KOH, pH 7.6, containing 400 mM sorbitol, 5 mM $MgCl_2$, and 2.5 mM EDTA. Isolated intact chloroplasts were suspended in 25 mM HEPES-KOH, pH 7.6, containing 3 mM $MgCl_2$. The insoluble fraction containing thylakoids and envelopes was separated from the stroma fraction by centrifugation at 10,000*g* for 3 min at 4°C.

SDS PAGE and Western Blot Analysis

Proteins were separated by SDS-PAGE using the conventional Laemmli (Tris-Gly) system (Laemmli, 1970) or using a Tris-tricine buffer system (for PGR5 detection; Schägger and von Jagow, 1987) and transferred onto polyvinylidene difluoride membranes. Specific antibodies against Trx-isoforms, SBPase, FBPase, NADP-malate dehydrogenase, CYP20-3, ATP synthase CF_1-ɣ (ATPC1), PGR5, and PGRL1 were prepared as described previously (Okegawa and Motohashi, 2015, 2016). For PsbA, PsbQ, PsaA, PsaF, violaxanthin deepoxidase (VDE), zeaxanthin epoxidase (ZEP), and PsbS, commercially available polyclonal antibodies (Agrisera) were used. Immunoblot signals were visualized using the Immobilon western chemiluminescent HRP substrate (EMD Millipore) or ECL Plus western blotting detection kit (GE Healthcare). The chemiluminescence was detected using a LAS-3000UV mini lumino-image analyzer (Fujifilm).

In Vitro Assay of Linear Electron Transport Activity

Measurement of linear electron transport activity was performed using isolated chloroplasts, as described previously (Munekage et al., 2002). Intact chloroplasts (20 μg mL^{-1}) were osmotically ruptured in 50 mM HEPES/NaOH, pH 7.6, containing 7 mM $MgCl_2$, 1 mM $MnCl_2$, 2 mM EDTA, 30 mM KCl, and 0.25 mM KH_2PO_4. Linear electron transport activity was determined based on the effective quantum yields of PSII [Y(II)] at 17 and 167 μmol photons m^{-2} s^{-1} using a mini-PAM portable chlorophyll fluorometer (Walz). Before measurement, the electron acceptors Spinach Fd (5 μM; Sigma) and $NADP^+$ (1 mM; Oriental Kobo) were added.

In Vivo Measurements of Chlorophyll Fluorescence and P700 Absorption Changes

Chlorophyll fluorescence was measured using a mini-PAM II portable chlorophyll fluorometer (Walz) for the analysis depicted in Figure 2. Minimum fluorescence (F_o) was obtained from the open PSII reaction centers in the dark-adapted state, using a weak measuring light (red light, 654 nm, 0.05–0.1 μmol photons m^{-2} s^{-1}). An SP of red light (800 ms, 3000 μmol photons m^{-2} s^{-1}) was applied to determine the maximum fluorescence with closed PSII centers in the dark-adapted state (F_m) and during illumination with red AL (F_m'). The steady-state fluorescence level (F_s) was recorded during red AL illumination. The F_v/F_m was calculated as $(F_m - F_o)/F_m$. Y(II) and NPQ were calculated as $(F_m' - F_s)/F_m'$ and $(F_m - F_m')/F_m'$, respectively (Genty et al., 1989). The value of qPd was calculated according to the method described by Ruban and Murchie (2012) as follows: $qPd = (F_m' - F_{o'act})/(F_m' - F_{o'calc})$, where $F_{o'calc} = 1/(1/F_o - 1/F_m + 1/F_m')$. Far-red light (737 nm) was used to determine F_o and $F_{o'act}$. qPd was induced by illumination at 50 μmol photons m^{-2} s^{-1} (growth light) for 15 min. Otherwise, chlorophyll fluorescence and chlorophyll P700 absorption changes in the PSI reaction center were measured simultaneously using a portable chlorophyll fluorometer (DUAL-PAM-100 [MODULAR version]

analyzer equipped with a P700 dual-wavelength emitter at 830 and 870 nm; Walz). The plants were kept in the dark for 30 min before each measurement, and detached leaves were used for the analysis. Red measuring light (620 nm) and AL (635 nm) were used for analysis. An SP of red light (300 ms, 10,000 μmol photons m^{-2} s^{-1}) was applied to determine F_m and F_m'.

The redox change of P700 was assessed by monitoring the absorbance changes to transmitted light at 830 and 875 nm. Pm (the level of the P700 signal of maximum oxidizable P700) was determined by the application of an SP in the presence of far-red light (720 nm). The maximal level of oxidized P700 during AL illumination (Pm′) was determined by SP application. The P700 signal P was recorded immediately before an SP. Y(I) was calculated as (Pm′ − P)/Pm. Y(NA) was calculated as (Pm − Pm′)/ Pm. Y(ND) was calculated as P/Pm. Three complementary quantum yields were defined as follows: Y(I) + Y(NA) + Y(ND) = 1 (Klughammer and Schreiber, 1994). The relative level of reduced P700 was calculated as 1 − Y(ND). The value can vary between 0 (P700 fully oxidized) and 1 (P700 fully reduced) in a given state.

ECS Analysis

The ECS measurements were carried out using the Walz dual-PAM 100 equipped with a P515/535 module. Each measurement was carried out in ambient air, using 4- to 5-week-old plants grown under long-day conditions that had been dark adapted for 30 min. It consisted of 5 min of red AL at 75 μmol photons m^{-2} s^{-1}; a 1-s dark pulse at each different time point was used to record ECS_t. This represented the size of the light-induced pmf and was estimated from the total amplitude of the rapid decay of the ECS signal during the dark pulse, as described previously (Wang et al., 2015). The ECS_t levels were normalized against a 515-nm absorbance change induced by a single turnover flash (ECS_{ST}), as measured in dark-adapted leaves before recording. This normalization allowed us to consider possible changes in leaf thickness and chloroplast density between leaves (Takizawa et al., 2008).

In Vivo Photoreduction of Thiol Enzymes

Photoreduction of Trx target enzymes in seedlings was determined using the free thiol-specific-modifying reagent 4-acetamido-4′-maleimidylstilbene-2,2′-disulfonic acid (Thermo Fisher Scientific) as described previously (Okegawa and Motohashi, 2015). Seedlings were dark adapted for 8 h and exposed to light (80 μmol photons m^{-2} s^{-1}) for up to 60 min. Samples were collected at the indicated time points and detected by western blot analysis. The reduction level of the proteins was quantified using Multi Gauge 3.1 software (Fujifilm) and presented as the ratio of reduced protein to total protein.

Statistical Analysis

Calculations were performed on more than three independent biological replicates (see figure legends). Tukey multiple comparisons test was used to determine significant differences among the materials tested ($P < 0.05$).

Accession Numbers

Sequence data from this article can be found in the Arabidopsis Genome Initiative or GenBank/EMBL databases under the following accession numbers: Trx *f*1 (At3g02730), Trx *f*2 (At5g16400), PGR1 (At4g03280), and PGR5 (At2g05620).

Supplemental Data

The following supplemental materials are available.

Supplemental Figure S1. Visible phenotypes of the wild type and *pgr1*, *pgr5*, *trx f1f2*, *pgr1 trx f1f2*, and *pgr5 trx f1f2* mutants.

Supplemental Figure S2. Light intensity dependence of PSI and PSII photosynthetic parameters in the wild type and *pgr1*, *pgr5*, *trx f1f2*, *pgr1 trx f1f2*, and *pgr5 trx f1f2* mutants.

Supplemental Figure S3. Simultaneous analysis of PSI and PSII photosynthetic parameters during steady-state photosynthesis.

Supplemental Figure S4. ECS analysis in the wild type and *pgr1*, *pgr5*, *trx f1f2*, *pgr1 trx f1f2*, and *pgr5 trx f1f2* mutants.

Supplemental Table S1. Primers used in this study.

ACKNOWLEDGMENTS

We thank Dr. Tsuyoshi Endo (Kyoto University) for providing PnsB1 antibody. The authors have no conflict of interest to declare.

Received June 8, 2020; accepted September 2, 2020; published September 11, 2020.

LITERATURE CITED

Avenson TJ, Cruz JA, Kanazawa A, Kramer DM (2005) Regulating the proton budget of higher plant photosynthesis. Proc Natl Acad Sci USA **102:** 9709–9713

Balsera M, Uberegui E, Schürmann P, Buchanan BB (2014) Evolutionary development of redox regulation in chloroplasts. Antioxid Redox Signal **21:** 1327–1355

Breyton C, Nandha B, Johnson GN, Joliot P, Finazzi G (2006) Redox modulation of cyclic electron flow around photosystem I in C3 plants. Biochemistry **45:** 13465–13475

Buchanan BB (2016) The path to thioredoxin and redox regulation in chloroplasts. Annu Rev Plant Biol **67:** 1–24

Carrillo LR, Froehlich JE, Cruz JA, Savage LJ, Kramer DM (2016) Multilevel regulation of the chloroplast ATP synthase: The chloroplast NADPH thioredoxin reductase C (NTRC) is required for redox modulation specifically under low irradiance. Plant J **87:** 654–663

Courteille A, Vesa S, Sanz-Barrio R, Cazalé AC, Becuwe-Linka N, Farran I, Havaux M, Rey P, Rumeau D (2013) Thioredoxin m4 controls photosynthetic alternative electron pathways in Arabidopsis. Plant Physiol **161:** 508–520

DalCorso G, Pesaresi P, Masiero S, Aseeva E, Schünemann D, Finazzi G, Joliot P, Barbato R, Leister D (2008) A complex containing PGRL1 and PGR5 is involved in the switch between linear and cyclic electron flow in *Arabidopsis*. Cell **132:** 273–285

Foyer CH, Lelandais M, Harbinson J (1992) Control of the quantum efficiencies of photosystems I and II, electron flow, and enzyme activation following dark-to-light transitions in pea leaves: Relationship between NADP/NADPH ratios and NADP-malate dehydrogenase activation state. Plant Physiol **99:** 979–986

Geigenberger P, Fernie AR (2014) Metabolic control of redox and redox control of metabolism in plants. Antioxid Redox Signal **21:** 1389–1421

Genty B, Briantais J-M, Baker NR (1989) The relationship between the quantum yield of photosynthetic electron transport and quenching of chlorophyll fluorescence. Biochim Biophys Acta Gen Subj **990:** 87–92

Hashimoto M, Endo T, Peltier G, Tasaka M, Shikanai T (2003) A nucleus-encoded factor, CRR2, is essential for the expression of chloroplast ndhB in Arabidopsis. Plant J **36:** 541–549

Horton P, Ruban AV, Walters RG (1996) Regulation of light harvesting in green plants. Annu Rev Plant Physiol Plant Mol Biol **47:** 655–684

Jahns P, Graf M, Munekage Y, Shikanai T (2002) Single point mutation in the Rieske iron-sulfur subunit of cytochrome b6/f leads to an altered pH dependence of plastoquinol oxidation in *Arabidopsis*. FEBS Lett **519:** 99–102

Johnson MP, Ruban AV (2014) Rethinking the existence of a steady-state $\Delta\psi$ component of the proton motive force across plant thylakoid membranes. Photosynth Res **119:** 233–242

Kang Z, Qin T, Zhao Z (2019) Thioredoxins and thioredoxin reductase in chloroplasts: A review. Gene **706:** 32–42

Klughammer C, Schreiber U (1994) An improved method, using saturating light pulses, for the determination of photosystem I quantum yield via P700+-absorbence changes at 830 nm. Planta **192:** 261–268

Klughammer C, Schreiber U (2008) Saturation pulse method for assessment of energy conversion in PSI. PAM Appl Notes **1:** 11–14

Laemmli UK (1970) Cleavage of structural proteins during the assembly of the head of bacteriophage T4. Nature **227:** 680–685

Li XP, Muller-Moule P, Gilmore AM, Niyogi KK (2002) PsbS-dependent enhancement of feedback de-excitation protects photosystem II from photoinhibition. Proc Natl Acad Sci USA **99:** 15222–15227

Livingston AK, Cruz JA, Kohzuma K, Dhingra A, Kramer DM (2010) An Arabidopsis mutant with high cyclic electron flow around photosystem

I (hcef) involving the NADPH dehydrogenase complex. Plant Cell **22:** 221–233

Müller P, Li XP, Niyogi KK (2001) Non-photochemical quenching. A response to excess light energy. Plant Physiol **125:** 1558–1566

Munekage Y, Hashimoto M, Miyake C, Tomizawa K, Endo T, Tasaka M, Shikanai T (2004) Cyclic electron flow around photosystem I is essential for photosynthesis. Nature **429:** 579–582

Munekage Y, Hojo M, Meurer J, Endo T, Tasaka M, Shikanai T (2002) PGR5 is involved in cyclic electron flow around photosystem I and is essential for photoprotection in *Arabidopsis*. Cell **110:** 361–371

Munekage Y, Takeda S, Endo T, Jahns P, Hashimoto T, Shikanai T (2001) Cytochrome b(6)f mutation specifically affects thermal dissipation of absorbed light energy in *Arabidopsis*. Plant J **28:** 351–359

Nakano H, Yamamoto H, Shikanai T (2019) Contribution of NDH-dependent cyclic electron transport around photosystem I to the generation of proton motive force in the weak mutant allele of pgr5. Biochim Biophys Acta Bioenerg **1860:** 369–374

Nalin CM, McCarty RE (1984) Role of a disulfide bond in the gamma subunit in activation of the ATPase of chloroplast coupling factor 1. J Biol Chem **259:** 7275–7280

Naranjo B, Diaz-Espejo A, Lindahl M, Cejudo FJ (2016) Type-f thioredoxins have a role in the short-term activation of carbon metabolism and their loss affects growth under short-day conditions in *Arabidopsis thaliana*. J Exp Bot **67:** 1951–1964

Nikkanen L, Rintamäki E (2019) Chloroplast thioredoxin systems dynamically regulate photosynthesis in plants. Biochem J **476:** 1159–1172

Nikkanen L, Toivola J, Rintamäki E (2016) Crosstalk between chloroplast thioredoxin systems in regulation of photosynthesis. Plant Cell Environ **39:** 1691–1705

Nikkanen L, Toivola J, Trotta A, Diaz MG, Tikkanen M, Aro EM, Rintamäki E (2018) Regulation of cyclic electron flow by chloroplast NADPH-dependent thioredoxin system. Plant Direct **2:** e00093

Okegawa Y, Kagawa Y, Kobayashi Y, Shikanai T (2008) Characterization of factors affecting the activity of photosystem I cyclic electron transport in chloroplasts. Plant Cell Physiol **49:** 825–834

Okegawa Y, Motohashi K (2015) Chloroplastic thioredoxin m functions as a major regulator of Calvin cycle enzymes during photosynthesis in vivo. Plant J **84:** 900–913

Okegawa Y, Motohashi K (2016) Expression of spinach ferredoxin-thioredoxin reductase using tandem T7 promoters and application of the purified protein for in vitro light-dependent thioredoxin-reduction system. Protein Expr Purif **121:** 46–51

Pérez-Ruiz JM, Spínola MC, Kirchsteiger K, Moreno J, Sahrawy M, Cejudo FJ (2006) Rice NTRC is a high-efficiency redox system for chloroplast protection against oxidative damage. Plant Cell **18:** 2356–2368

Porra R, Thompson W, Kriedemann P (1989) Determination of accurate extinction coefficients and simultaneous equations for assaying chlorophylls a and b extracted with four different solvents: Verification of the concentration of chlorophyll standards by atomic absorption spectroscopy. Biochim Biophys Acta Bioenerg **975:** 384–394

Ruban AV, Murchie EH (2012) Assessing the photoprotective effectiveness of non-photochemical chlorophyll fluorescence quenching: A new approach. Biochim Biophys Acta **1817:** 977–982

Schägger H, von Jagow G (1987) Tricine-sodium dodecyl sulfate-polyacrylamide gel electrophoresis for the separation of proteins in the range from 1 to 100 kDa. Anal Biochem **166:** 368–379

Schürmann P, Buchanan BB (2008) The ferredoxin/thioredoxin system of oxygenic photosynthesis. Antioxid Redox Signal **10:** 1235–1274

Schwarz O, Schürmann P, Strotmann H (1997) Kinetics and thioredoxin specificity of thiol modulation of the chloroplast H+-ATPase. J Biol Chem **272:** 16924–16927

Serrato AJ, Pérez-Ruiz JM, Spínola MC, Cejudo FJ (2004) A novel NADPH thioredoxin reductase, localized in the chloroplast, which deficiency causes hypersensitivity to abiotic stress in *Arabidopsis thaliana*. J Biol Chem **279:** 43821–43827

Shikanai T, Yamamoto H (2017) Contribution of cyclic and pseudo-cyclic electron transport to the formation of proton motive force in chloroplasts. Mol Plant **10:** 20–29

Stiehl HH, Witt HT (1969) Quantitative treatment of the function of plastoquinone in phostosynthesis. Z Naturforsch B **24:** 1588–1598

Suorsa M, Järvi S, Grieco M, Nurmi M, Pietrzykowska M, Rantala M, Kangasjärvi S, Paakkarinen V, Tikkanen M, Jansson S, et al (2012) PROTON GRADIENT REGULATION5 is essential for proper acclimation of Arabidopsis photosystem I to naturally and artificially fluctuating light conditions. Plant Cell **24:** 2934–2948

Takizawa K, Kanazawa A, Kramer DM (2008) Depletion of stromal P(i) induces high 'energy-dependent' antenna exciton quenching (q(E)) by decreasing proton conductivity at CF(O)-CF(1) ATP synthase. Plant Cell Environ **31:** 235–243

Thormählen I, Meitzel T, Groysman J, Öchsner AB, von Roepenack-Lahaye E, Naranjo B, Cejudo FJ, Geigenberger P (2015) Thioredoxin f1 and NADPH-dependent thioredoxin reductase C have overlapping functions in regulating photosynthetic metabolism and plant growth in response to varying light conditions. Plant Physiol **169:** 1766–1786

Thormählen I, Ruber J, von Roepenack-Lahaye E, Ehrlich SM, Massot V, Hümmer C, Tezycka J, Issakidis-Bourguet E, Geigenberger P (2013) Inactivation of thioredoxin f1 leads to decreased light activation of ADP-glucose pyrophosphorylase and altered diurnal starch turnover in leaves of *Arabidopsis* plants. Plant Cell Environ **36:** 16–29

Tikhonov AN (2013) pH-dependent regulation of electron transport and ATP synthesis in chloroplasts. Photosynth Res **116:** 511–534

Tikhonov AN (2015) Induction events and short-term regulation of electron transport in chloroplasts: An overview. Photosynth Res **125:** 65–94

Wang C, Yamamoto H, Shikanai T (2015) Role of cyclic electron transport around photosystem I in regulating proton motive force. Biochim Biophys Acta **1847:** 931–938

Wang P, Liu J, Liu B, Feng D, Da Q, Wang P, Shu S, Su J, Zhang Y, Wang J, et al (2013) Evidence for a role of chloroplastic m-type thioredoxins in the biogenesis of photosystem II in Arabidopsis. Plant Physiol **163:** 1710–1728

Wilson S, Ruban AV (2019) Quantitative assessment of the high-light tolerance in plants with an impaired photosystem II donor side. Biochem J **476:** 1377–1386

Yamamoto H, Shikanai T (2019) PGR5-dependent cyclic electron flow protects photosystem I under fluctuating light at donor and acceptor sides. Plant Physiol **179:** 588–600

Yamamoto H, Shikanai T (2020) Does the Arabidopsis *proton gradient regulation5* mutant leak protons from the thylakoid membrane? Plant Physiol **184:** 421–427

Yoshida K, Hara S, Hisabori T (2015) Thioredoxin selectivity for thiol-based redox regulation of target proteins in chloroplasts. J Biol Chem **290:** 14278–14288

Yoshida K, Yokochi Y, Hisabori T (2019) New light on chloroplast redox regulation: Molecular mechanism of protein thiol oxidation. Front Plant Sci **10:** 1534